Global drivers of avian haemosporidian infections vary across zoogeographical regions

Alan Fecchio[1], Nicholas J. Clark[2], Jeffrey A. Bell[3], Heather Skeen[4], Holly L. Lutz[5], Gabriel M. De La Torre[6], Jefferson A. Vaughan[3], Vasyl V. Tkach[3], Fabio Schunck[7], Francisco C. Ferreira[8], Érika M. Braga[9], Camile Lugarini[10], Wanyoike Wamiti[11], Janice H. Dispoto[12], Spencer C. Galen[13], Karin Kirchgatter[14], M. Cecilia Sagario[15], Victor R. Cueto[16], Daniel González-Acuña[17], Mizue Inumaru[18], Yukita Sato[18], Yvonne R. Schumm[19], Petra Quillfeldt[19], Irene Pellegrino[20], Guha Dharmarajan[21], Pooja Gupta[21], V. V. Robin[22], Arif Ciloglu[23], Alparslan Yildirim[23], Xi Huang[24], Leonardo Chapa-Vargas[25], Paulina Álvarez Mendizábal[26], Diego Santiago-Alarcon[26,27], Sergei V. Drovetski[28], Olof Hellgren[29], Gary Voelker[30], Robert E. Ricklefs[31], Shannon Hackett[32], Michael D. Collins[33], Jason D. Weckstein[12,34] Konstans Wells[35]

[1] Programa de Pós-graduação em Ecologia e Conservação da Biodiversidade, Universidade Federal de Mato Grosso, Cuiabá, MT 78060900, Brazil

[2] School of Veterinary Science, University of Queensland, Gatton, Queensland, Australia

[3] Department of Biology, University of North Dakota, Grand Forks, ND 58201, USA

[4] Committee on Evolutionary Biology, University of Chicago, Chicago, IL, 6063 and Negaunee Integrative Research Center, The Field Museum, Chicago, IL, 60605 USA

[5] Department of Surgery, University of Chicago, 5812 S. Ellis Ave., Chicago, IL 60637 and Integrative Research Center, Field Museum of Natural History, 1400 South Lake Shore Drive, Chicago, IL 60605 USA

[6] Programa de Pós-graduação em Ecologia e Conservação, Universidade Federal do Paraná, Curitiba, PR, Brazil

[7] Brazilian Committee for Ornithological Records – CBRO

[8] Center for Conservation Genomics, Smithsonian Conservation Biology Institute, Washington, DC, USA

[9] Departamento de Parasitologia, Universidade Federal de Minas Gerais, Belo Horizonte, MG 31270-901, Brazil

[10] Centro Nacional de Pesquisa e Conservação de Aves Silvestres, Instituto Chico Mendes de Conservação da Biodiversidade, Florianópolis, SC, Brazil

[11] Zoology Department, National Museums of Kenya, P.O. Box 40658-00100, Nairobi, Kenya

[12] Department of Ornithology, Academy of Natural Sciences of Drexel University, Philadelphia, PA 19103, USA

[13] Biology Department, University of Scranton, Scranton, PA, USA

[14] Laboratório de Bioquímica e Biologia Molecular, Superintendência de Controle de Endemias, São Paulo, SP 01027-000 and Instituto de Medicina Tropical, Faculdade de Medicina, Universidade de São Paulo, São Paulo, SP 05403-000, Brazil

[15] Grupo de Ecología Terrestre de Neuquén, Instituto de Investigaciones en Biodiversidad y Medioambiente (INIBIOMA–CONICET and UNComahue), and Centro de Ecología Aplicada del Neuquén (CEAN), Junín de los Andes, CP8371, Neuquén, Argentina

[16] Centro de Investigación Esquel de Montaña y Estepa Patagónica (CIEMEP), CONICET – Universidad Nacional de la Patagonia San Juan Bosco, Esquel, Chubut, Argentina

[17] Laboratorio de Parásitos y Enfermedades de Fauna Silvestre, Facultad de Ciencias Veterinarias, Universidad de Concepción, Avenida Vicente Méndez 595, Chillán, Chile

[18] Laboratory of Biomedical Science, Department of Veterinary Medicine, College of Bioresource Sciences, Nihon University, Fujisawa 252-0880, Japan

[19] Department of Animal Ecology & Systematics, Justus Liebig University Giessen, Heinrich-Buff-Ring 26, D-35392, Giessen, Germany

[20] Department of Science and Technological Innovation, University of Piemonte Orientale, Viale Teresa Michel 11, 15121, Alessandria, Italy

[21] Savannah River Ecology Laboratory, University of Georgia, Aiken, SC, USA

[22] Indian Institute of Science Education and Research Tirupati, Mangalam, Tirupati 517507, India

[23] Department of Parasitology, Faculty of Veterinary Medicine and Vectors and Vector-Borne Diseases Implementation and Research Center, Erciyes University, Kayseri 38280, Turkey

[24] MOE Key Laboratory for Biodiversity Science and Ecological Engineering, College of Life Sciences, Beijing Normal University, Beijing 100875, China

[25] Instituto Potosino de Investigación Científica y Tecnológica, A.C. - CONACYT. 78216 San Luis Postosí. San Luis Potosí, Mexico

[26] Instituto de Ecología, A.C. - CONACYT. 91073 Xalapa. Veracruz, Mexico

[27] Department of Integrative Biology, University of South Florida, Tampa, FL 33620, USA

[28] U.S. Geological Survey, Eastern Ecological Science Center at Patuxent Research Refuge, Beltsville, MD 20705, USA

[29] MEMEG, Department of Biology, Lund University, Sweden

[30] Department of Ecology and Conservation Biology, Texas A&M University, College Station, TX, USA

[31] Department of Biology, University of Missouri-St. Louis, St. Louis, MO 63121, USA

[32] The Richard and Jill Chaifetz Associate Curator of Birds, Life Sciences and Pritzker Lab Field Museum of Natural History, 1400 South Lake Shore Drive, Chicago, IL 60605, USA

[33] Department of Biology, Rhodes College, Memphis, TN 38112, USA

[34] Department of Biodiversity, Earth, and Environmental Sciences, Drexel University, Philadelphia, PA 19103, USA

[35] Department of Biosciences, Swansea University, Swansea, SA2 8PP UK

Correspondence

Alan Fecchio, ORCID https://orcid.org/0000-0002-7319-0234

Programa de Pós-Graduação em Ecologia e Conservação da Biodiversidade,

Universidade Federal de Mato Grosso,

Avenida Fernando Corrêa da Costa 2367, Cuiabá, MT, 78060900, Brazil

E-mail: alanfecchio@gmail.com

Running title

Global drivers of avian haemosporidian prevalence

Acknowledgments

We dedicate this research to our colleague Daniel González-Acuña, who died during completion of this manuscript. We thank all ornithologists and field assistants who helped collect avian tissue samples used in this study, as well as all collaborators who contributed previously published data. We are grateful to Staffan Bensch for providing data from Sweden and to Vincenzo Ellis for providing data from eastern USA. The curators and collection managers from the following museums loaned new samples used in this study: Academy of Natural Sciences of Drexel University, Field Museum of Natural History, and Yale Peabody Museum of Natural

History. We also thank government agencies that provided permits necessary for collection and exportation of tissue samples. Any use of trade, firm, or product names is for descriptive purposes only and does not imply endorsement by the U.S. Government.

Data availability statement

The bird infection data used in this study are available as Supporting Information Table S1. R code to retrieve publicly available environmental and species trait data, and perform the analysis is available from https://github.com/konswells1/Global-haemosporidian-prevalence.

Biosketch

We have worked as a team to characterize local and regional datasets of avian haemosporidian assemblages for a global synthesis. This study represents the efforts of a broad range of researchers from different disciplines: ecologists, entomologists, molecular biologists, ornithologists, and parasitologists interested in factors that shape the prevalence and distribution of parasitic organisms in avian hosts worldwide.

Funding

This work was funded in part by U. S. National Science Foundation grants DEB-1503804 to JDW, DEB-1120734 to VVT, and DEB 1717498 to FCF. Additional support was received from the Field Museum's Emerging Pathogens Project, with funding by The Davee Foundation and The Dr. Ralph and Marian Falk Medical Research Trust. DS-A was funded by Consejo Nacional de Ciencia y Tecnología (CONACYT, project number Ciencia Básica 2011-01-168524 and project number Problemas Nacionales 2015-01-1628). DGA was financed by project FONDECYT Nº1170972. WW was funded by Wilson Ornithological Society (Hall/Mayfield

Research Grant), British Ecological Society (Ecologists in Africa No. EA16/1083), and African Council of the Field Museum, Chicago. GD acknowledges support from the U.S. Department of Energy and the Department of Science and Technology, India. RER was supported by grants from the National Geographic Society and the U. S. National Science Foundation. AF was supported by a PNPD scholarship from Coordenação de Aperfeiçoamento de Pessoal de Nível Superior - CAPES (Process number 88887.342366/2019-00). KK is a CNPq research fellow (process number 308678/2018-4). KW acknowledges support from the Supercomputing Wales project, which is partly funded by the European Regional Development Fund (ERDF) via the Welsh Government.

Author contributions

AF, KW, and NJC conceived the idea, designed the research, analysed the data, and wrote the manuscript; the remaining authors contributed with avian tissue collection, sample screening, data curation, and funding reagents and field expeditions. All authors contributed critically to the manuscript drafts and gave final approval for publication.

Abstract

Aim: Macroecological analyses provide valuable insights into factors that influence how parasites are distributed across space and among hosts. Amid large uncertainties that arise when generalizing from local and regional findings, hierarchical approaches applied to global datasets are required to determine whether drivers of parasite infection patterns vary across scales. We assessed global patterns of haemosporidian infections across a broad diversity of avian host

clades and zoogeographical realms to depict hotspots of prevalence and to identify possible underlying drivers.

Location: Global.

Time period: 1994-2019

Major taxa studied: Avian haemosporidian parasites (genera *Plasmodium*, *Haemoproteus*, *Leucocytozoon*, and *Parahaemoproteus*).

Methods: We amalgamated infection data from 53,669 individual birds representing 2,445 species worldwide. Spatio-phylogenetic hierarchical Bayesian models were built to disentangle potential landscape, climatic, and biotic drivers of infection probability while accounting for spatial context and avian host phylogenetic relationships.

Results: Idiosyncratic responses of the three most common haemosporidian genera to climate, habitat, host relatedness, and host ecological traits indicated marked variation in host infection rates from local to global scales. Notably, host ecological drivers, such as migration distance for *Plasmodium* and *Parahaemoproteus*, exhibited predominantly varying or even opposite effects on infection rates across regions, whereas climatic effects on infection rates were more consistent across realms. Moreover, infections in some low-prevalence realms were disproportionately concentrated in a few local hotspots, suggesting that regional-scale variation in habitat and microclimate may influence transmission in addition to global drivers.

Main conclusions: Our hierarchical global analysis supports regional-scale findings showing the synergistic effects of landscape, climate, and host ecological traits on parasite transmission for a cosmopolitan and diverse group of avian parasites. Our results underscore the need to account for such interactions, as well as possible variation in drivers across regions, to produce the robust inference required to predict changes in infection risk under future scenarios.

Keywords: avian malaria, avian migration, disease hotspot, disease macroecology, haemosporidian prevalence, host-parasite interaction, infection probability, parasite macroecology, *Plasmodium*, spatio-phylogenetic models

Introduction

A growing consensus based on theory and empirical evidence suggests that global change will impact the worldwide distributions and burdens of vector-transmitted pathogens that infect humans (Lafferty, 2009; Ryan, Carlson, Mordecai, & Johnson, 2019; Mordecai, Ryan, Caldwell, Shah, & LaBeaud, 2020). Likewise, climate change and anthropogenic landscape modification are predicted to alter the geographic range of non-human pathogens, such as avian malaria parasites (Benning, LaPointe, Atkinson, & Vitousek, 2002; Loiseau et al., 2012, 2013; Pérez-Rodríguez, de la Hera, Fernández-González, & Pérez-Tris, 2014), whereby infection patterns of avian hosts in natural environments are often driven by an interplay of regional changes in biotic and abiotic conditions (Fecchio et al., 2019). Anticipating spatial or temporal shifts in infection risk requires reliable estimates of prevalence across habitats under different anthropogenic

disturbance levels and climatic gradients (Stephens et al., 2016; Weiss et al., 2019). The synergistic effects of such drivers on the broadest levels of host taxonomic and community organisation are poorly described for the majority of non-human parasites.

Mean temperatures are expected to increase unevenly across the globe in the coming decades (Wehner, 2020). For example, nights are expected to be warmer in continental interiors than in coastal regions (Wehner, 2020), and extreme temperature ranges are expected to decrease at high-latitudes and increase within subtropical regions (Fischer, Lawrence, & Sanderson, 2011). As the effects of climate-driven temperature change will not be spatially uniform, average global warming could alter disease transmission rates and shift the geographic ranges of many parasitic organisms with different modes of transmission (Altizer, Ostfeld, Johnson, Kutz, & Harvell, 2013; Loiseau et al., 2013). For example, optimal temperatures for reproduction of *Plasmodium* malaria parasites within invertebrate vectors are a critical prerequisite for successful transmission to humans (Mordecai et al., 2013). The existence of thermal niches that promote vector activity means that distributions of many vector-borne pathogens may extend into new geographical regions as temperatures change (Ryan et al., 2019). In Africa, for example, where average temperatures are expected to increase between 3°C and 4°C by 2100 (roughly 1.5 times the global mean response; Christensen et al., 2007), hotspots for human malaria risk are predicted to shift toward higher elevations and the relative burdens of dengue fever over malaria are expected to increase across the Sub-Saharan region (Mordecai et al., 2020). Given that temperature might predominately influence infection risk for vector-transmitted pathogens, future climate warming will be an important force driving the prevalence of many human and wildlife diseases (Benning et al., 2002; Lafferty, 2009; Loiseau et al., 2013; Cable et al., 2017).

For those parasites infecting multiple host species, spatial heterogeneity in infection probability across host communities may change in response not only to climate filters, but also to changing host species distributions (e.g., host richness) that provide new ecological opportunities for a parasite to expand its host range and increase its local prevalence (Canard et al., 2014; Wells & Clark, 2019). Inevitably, transformation of natural habitats for urban development and agriculture is creating widespread change in habitats and microclimates, leading to shifts in host and vector species pools, thereby impacting parasite transmission (Ferraguti, Hernández-Lara, Sehgal, & Santiago-Alarcon, 2020). This human-induced habitat modification is occurring unevenly across regions and most rapidly within tropical and subtropical grasslands, savannahs, and shrubland ecosystems (Williams et al., 2020).

At the avian host-species level, functional traits, such as preferred foraging habitat or dependence on forested habitats (e.g., higher vegetation density), and foraging height, can influence rates of vector exposure for a given avian host, leading to heterogeneous infection probabilities across avian species (Garvin & Greiner, 2003; Clark, Drovetski, & Voelker, 2020). However, assessing the influence of host and parasite traits on infection rates across host communities requires careful consideration of species' evolutionary histories. Traits that influence avian host immune responses and potentially restrict parasite invasion, such as body size (Ruhs, Martin, & Downs, 2020), are often phylogenetically conserved (Minias, 2019). Accordingly, one would expect greater variation in infection rates among rather than within host clades. Furthermore, avian life-history strategy is known to influence haemosporidian prevalence (Lutz et al., 2015; Barrow et al., 2019; Ellis, Fecchio, & Ricklefs, 2020). For example, larger and migratory avian species are more often infected by haemosporidian parasites, due to their propensity to harbor a broader diversity of parasite lineages or by being exposed to a higher

abundance and diversity of vectors and, in turn, to vector-transmitted parasites (Filion, Eriksson, Jorge, Niebuhr, & Poulin, 2020; de Angeli Dutra, Fecchio, Braga, & Poulin, 2021).

Avian haemosporidian parasites of the genera *Plasmodium*, *Haemoproteus*, *Parahaemoproteus*, and *Leucocytozoon* comprise a diverse group of vector-transmitted parasites (Valkiūnas, 2005; Galen et al., 2018). They infect blood cells of a wide range of avian hosts across all zoogeographic regions (Valkiūnas, 2005). The parasite genera *Plasmodium*, *Haemoproteus*, *Parahaemoproteus*, and *Leucocytozoon* are predominantly transmitted by mosquitos (Culicidae), hippoboscid flies (Hippoboscidae), biting midges (Ceratopogonidae), and black flies (Simuliidae), respectively (reviewed by Santiago-Alarcon, Palinauskas, & Schaefer, 2012). The life histories of these dipteran vectors depend on temperature and on the presence of either running or standing water (Valkiūnas, 2005; Santiago-Alarcon et al., 2012). Blackfly larval development and *Leucocytozoon* sexual reproduction do not appear to be highly constrained by low temperature (Valkiūnas, 2005; Fecchio et al., 2020). In contrast, the expected optimum temperature range of 13-28ºC for *Plasmodium* sexual reproduction and mosquito activity suggests some constraint on the transmission of avian malarial parasites along latitudinal or elevational gradients, despite *Plasmodium*'s global distribution (Valkiūnas, 2005; Santiago-Alarcon et al., 2012; Atkinson et al., 2014).

Haemosporidian parasites exhibit broad variation in prevalence, but the drivers of this variation across zoogeographical realms and among avian clades are only partially understood from region-level studies. In recent years, numerous studies have explored haemosporidian infection rates in birds across habitat gradients under different regional land use or climate conditions but with no consistent predictor identified across studies (e.g., Lutz et al., 2015; Ishtiaq, Bowden, & Jhala, 2017; Harvey & Voelker, 2019; Santiago-Alarcon et al., 2019; Ellis et

al., 2020; Gupta, Vishnudas, Robin, & Dharmarajan, 2020). Mounting evidence that various landscape and climate conditions, as well as host and vector species attributes, may drive avian haemosporidian infections calls for global approaches to disentangle abiotic and biotic drivers and anticipate macroecological patterns of parasite spread under current and future conditions.

To explore macroecological patterns of avian haemosporidian prevalence, we compiled global-scale infection data from 53,669 birds sampled from 141 avian families and 48 countries dispersed across 10 zoogeographical realms. First, we used 14 biotic and abiotic factors known to influence infection rates of haemosporidian parasites from multiple regional-scale studies to identify the drivers of infection probability for each parasite genus. Second, we assessed whether estimated effects of these drivers vary across zoogeographical realms. Third, we tested whether parasite prevalence varies among and within avian host clades. Our use of Bayesian hierarchical spatio-phylogenetic modelling to estimate prevalence at the broadest levels of host taxonomic and community organization across 10 zoogeographical realms, coupled with information on host species traits, allowed us to assess empirically how recent anthropogenic landscape transformations and climatic gradients synergistically drive the prevalence of a multi-host vector-transmitted group of parasites worldwide.

Materials and methods

Host-parasite data

To compile a representative global data set, we amalgamated field data from an international network of collaborators. We iteratively screened the available literature for studies reporting haemosporidian parasite prevalence. We screened the MalAvi database, the dominant public repository for avian malaria and related parasites (Bensch, Hellgren, & Pérez-Tris, 2009),

for studies reporting haemosporidian infection and parasite sequences in bird assemblages with reasonably sample sizes (> 100 individuals and > 5 host species). The raw capture data, including presence-absence records of infections and geographical coordinates of surveyed birds, were then requested from authors of relevant studies (see **Supporting Information Appendix S1** for further details). The compiled infection data can be accessed in **Supporting Information Table S1**.

Any compiled dataset is a finite and biased sample, given that study locations are chosen by researchers according to interest and logistic constraints rather than comprising a truly random sample. Nonetheless, we believe that our dataset provides a reasonable sample for exploring global patterns of haemosporidian infection in birds as it covers all major geographical regions (see **Supporting Information Table S2** for an overview of sample sizes from different zoogeographical regions). Moreover, our dataset includes ~24% of all known bird species (2,445 out of ~10,000 species recognized in Jetz, Thomas, Joy, Hartmann, & Mooers, 2012) and, to the best of our knowledge, covers the majority of areas surveyed for haemosporidian parasites in birds to date (**Supporting Information Figure S1**).

Bird species names from field data were revised and assigned to families according to the taxonomy used by Birdtree.org (Jetz et al., 2012). To generate a family-level phylogenetic tree, we randomly selected five species-level fossil-calibrated trees from a phylogenetic posterior distribution estimated from multiple genetic loci for the majority of extant bird species (Jetz et al., 2012). We calculated the pairwise mean Euclidean distance from all combinations of species for each pair of bird families and then converted the resulting distance matrix into a phylogenetic dendrogram using functions in the *ape* and *phylogram* R packages (Paradis, Claude, & Strimmer, 2004).

300

301 ***Parasite detection and identification***

302 Blood or tissue samples (liver or muscle) from all individuals were screened for
303 haemosporidian infection by PCR, following standard protocols for amplifying a fragment of the
304 parasite cytochrome-*b* gene (cyt-*b*). See **Supporting Information Appendix S1** for a detailed
305 description of the molecular detection of parasites.

306 Detected haemosporidian parasites were classified as *Haemoproteus*, *Leucocytozoon*,
307 *Parahaemoproteus*, or *Plasmodium* following the lineage identification protocol from the
308 MalAvi database (Bensch et al., 2009). We characterised each individual bird with respect to
309 each parasite genus as infected, not infected (screened with relevant primers but no lineage
310 detected) and missing (when the sample was not screened for the genus *Leucocytozoon* or when
311 separation of parasites of the genera *Haemoproteus* and *Plasmodium* was not achieved via
312 sequencing).

313

314 ***Host traits, climatic, and environmental data***

315 Relevant climatic variables at sample locations were obtained from the WorldClim
316 database of gridded climate data at a 0.01 degree resolution (Fick & Hijmans, 2017; http://world
317 clim.org/version2). We used annual mean temperature (bio1), annual rainfall (bio12), rainfall of
318 driest month (bio14), and rainfall seasonality (coefficient of variation in rainfall over the year,
319 bio15) to characterize aspects of climate previously shown to be associated with haemosporidian
320 occurrence (Fecchio et al., 2019; Clark et al., 2020). Elevation for all locations was quantified
321 using Shuttle Radar Topography Mission (SRTM) data, accessible through the *raster* package in
322 R. We classified the proportion of cover with forest and wetland in buffers of 10 km radius

around sample locations based on Copernicus landcover data from 2010 (map version 2.07; https://cds.climate.copernicus.eu). We downloaded the normalized difference vegetation index (NDVI) for the year 2010 in buffers of 10 km radius around all sampling locations from the Terra Moderate Resolution Imaging Spectroradiometer (MODIS, MOD13Q1 version 6, https://lpdaac.usgs.gov/products/mod13q1v006/) and calculated the mean and 1 standard deviation of NDVI as measures of the vegetation density and its annual fluctuation.

We defined local species richness of terrestrial birds based on a published map that summarizes bird species richness from BirdLife International range maps (https://biodiversitymapping.org/). Zoogeographical realm characterisation followed Holt et al. (2013), who delineated realms for birds by integrating the distributions and phylogenetic relationships of 10,074 bird species (see Holt et al., 2013).

We obtained species-level host traits from the EltonTraits v1.0 database (Wilman et al., 2014). In particular, we considered host body mass and the proportion of time individuals forage in the upper canopy, following previous trait-based analyses (Clark et al., 2020; Fecchio et al., 2020; Filion et al., 2020). For species with missing attributes in this database, values for the closest relative were used instead. We also included migration distance, extracted from Dufour et al. (2020), as a covariate. Species' migration distances were estimated from distribution maps (distance between midpoints of breeding and wintering ranges). As ages of individual birds were not available for all datasets, we did not include this trait in our model. We tested the 14 covariates for collinearity and found no strong correlation between predictor variables (all pairwise Spearman's $|r| < 0.7$).

Spatio-phylogenetic statistical modelling of multi-host infection patterns

To identify key drivers of infection of birds by haemosporidian parasites, while accounting for possible spatio-temporal and phylogenetic patterns underpinning the global dataset, we used a Bayesian statistical model to jointly estimate the posterior distributions of fixed parameters (host traits and environmental data as described above) and random effect parameters. This approach enabled us to reduce possible bias of modelled random effects in our multiple-species system, including the spatial clustering of samples (i.e., multiple host individuals captured under the same climate and habitat conditions), phylogenetic relationships of multiple species (i.e., bird species belonging to different families, which vary in sampling intensity and are unevenly clustered among sampling locations), temporal bias (i.e., samples collected in different years), and possible statistical interactions between these factors and zoogeographical region (i.e., when the effect of a factor differs across regions).

We assumed that infection *Y* of any sampled bird individual *i* with one of the haemosporidian genera *p* was a random draw from the true underlying parasite prevalence φ conditional on location *l* and host species identity *h*:

$$Y_{i,p} = \sim \text{Bernoulli}(\varphi_{i,l,h}) \quad \text{(eqn. 1)}$$

Within our generalized linear mixed-effect model (GLMM) framework, $\varphi_{i,l,h}$ was modelled further with a suitable link function (e.g., logit-link) and regressed against a range of location- and host-specific covariates (X_i and X_j; see descriptions in paragraph above), which we considered as fixed effects. In multi-species models, phylogenetic relationships likely influence conclusions on infection patterns, as closely related species often exhibit similar infection rates. We considered phylogenetic relationship of host species at the family-level as a random effect.

We considered four different model structures of increasing complexity to model logit($\varphi_{i,l,h}$) (see equations 2-5). First, in addition to the fixed effects, we considered sampling year, sampling source (τ_S with the three categories blood, muscle, and liver), and phylogenetic position as additional random effects, resulting in a phylogenetic GLMM (phyl-cov-GLMM) given as

$$\text{logit}(\varphi_{i,l,h}) \sim \beta_i X_{i,l} + \beta_j X_{j,h} + \gamma_y + \tau_S + v_F \quad \text{(eqn. 2)}$$

Here, β_i and β_j are the respective coefficient estimates for fixed effects, and γ_y is a random effect estimate based on sampling year. The random effect for phylogenetic relationships of different host species (v_F) is based on an inverse phylogenetic variance-covariance matrix derived from the pair-wise distance relationships (i.e., each sampled bird individual is characterised by its distance relationship in terms of its family to that of any other sampled bird individual), which can be expressed as latent Gaussian Markov random fields in Bayesian frameworks (we used the default 'generic0' option in the INLA package in R, which set the log-Gamma hyperparameter prior to a shape parameter of 1 and a rate of 0.00005). This option is equivalent to assuming that parameter estimates are derived from multivariate Gaussian distributions with (zero) means as hyper-parameters and spatially structured covariance matrices based on the underpinning dependence structure of distance/similarity relationships.

As our data set included samples from different zoogeographical realms with distinct host species assemblages, we tested a second model by including zoogeographical realm as a random effect (π_r), extending our basic phylogenetic GLMM (regional phyl-GLMM):

$$\text{logit}(\varphi_{i,l,h}) \sim \beta_i X_{i,l} + \beta_j X_{j,h} + \gamma_y + \tau_S + \pi_r + v_F \quad \text{(eqn. 3)}$$

Because captures of multiple host individuals at the same sampling locations in field surveillance leads to spatial pseudo-replication, we included a spatial random effect (u_l) in a fourth model, resulting in a spatio-phylogenetic GLMM (spatio-phyl-GLMM) given as:

$$\text{logit}(\varphi_{i,l,h}) \sim \beta_i X_{i,l} + \beta_j X_{j,h} + \gamma_y + \tau_S + \pi_r + v_F + u_l \quad \text{(eqn. 4)}$$

As an additional extension of the model, the fifth structure we explored included possible varying coefficient estimates for the fixed effects, assuming that because of the global scale of the study, drivers of infection probabilities (denoted as fixed effects) might vary across zoogeographical realms. Without loss of generality of the GLMM concept, we can assume that the fixed effect coefficient estimates β_i and β_j are not constant across zoogeographical realms, and they allow for possible deviation by modelling coefficients for each zoogeographical realm based on baseline values β_{0i} and β_{0j}, respectively. Moreover, random deviation from these values across samples from different zoogeographical realms *r*, result in a spatio-phylogenetic varying coefficient GLMM (spatio-phyl-varcoef-GLMM) given as:

$$\text{logit}(\varphi_{i,l,h}) \sim (\beta_{0i}+\xi_{i,r})X_{i,l} + (\beta_{0j}+\xi_{j,r})X_{j,h} + \gamma_y + \tau_S + \pi_r + v_F + u_l \quad \text{(eqn. 5)}$$

where $\xi_{i,r}$ and $\xi_{j,r}$ are vectors of random effects ($r = 1, \ldots, R$) defining a stochastic process with a specified Gaussian model over the R = 10 zoogeographical realms covered in this study.
In addition to the models described above, we fitted an intercept-only model to derive estimates of overall infection probability. We also fitted GLMMs with either realm or location as a random

effect to derive location- and region-specific estimates of infection probabilities. We do so to identify possible regional/local hotspots (average high infection probabilities). For model fitting and inference, we used the Integrated Nested Laplace Approximation (INLA) as a computationally efficient way to solve such latent Gaussian spatial models (Rue, Martino, & Chopin, 2009; Lindgren, Rue, & Lindstrøm, 2011). The INLA program models covariance for a random effect using a precision matrix (the inverse of a covariance matrix), taking advantage of sparse structures for efficient computation (Rue et al., 2009). For all random effects based on groupings (i.e., year, region, and region-level varying coefficients), we fitted first-order random walk models (Gaussian Markov Random Field, specified by a zero mean multivariate Gaussian probability density function).

For fitting the spatial random effect, u_l, we used the Stochastic Partial Differential Equation (SPDE) approach, as implemented in INLA, to model spatial effects using a Gaussian field based on a Matérn correlation function and a spatial triangulate mesh around sampling locations (Bakka et al., 2018). Setting the minimum allowed distance between points (cut-off) to 0.1 degree of latitude and the largest allowed triangle edge length (max edge) to 3 resulted in a mesh of 38,305 triangles, with the smallest edge lengths and finest mesh resolution adjacent to sampling locations (**Supporting Information Figure S2)**.

Continuous predictor variables were standardized to unit variance before analysis. For fixed effects, we used penalized complexity priors (using the 'pc.prec' option in the INLA settings), which penalize any departure from the base model and constrain coefficients to zero if there is insufficient support in the data otherwise. Such priors are commonly used for regularization of regression coefficients in multiple regression models (Simpson, Rue, Riebler, Martins, & Sørbye, 2017).

For model comparison and validation, we computed deviance information criteria (DIC) for each candidate model (Spiegelhalter, Best, Carlin, & van der Linde, 2002). We also computed conditional predictive ordinates (CPO) as cross-validation criteria, which estimate for each observation a probability of obtaining the observed value when the model is fitted using all data apart from the left-out observation; larger values indicate a better model fit to the data, whereas small values indicate a poorer model fit.

We present results as posterior means and 95% credible intervals (CIs) and considered CIs that did not overlap with zero or with each other in pairwise comparisons as 'significantly different'. Despite the overall large sample size, group-specific estimates can be burdened by substantial uncertainty (i.e., when few individuals for a certain location or host clade have been sampled). We considered group-level estimates to be meaningful only if the width of the respective CI was smaller than 10%.

Results

Strong spatial variation in haemosporidian infection probability coincides with strong phylogenetic variation among host clades

The estimated global average infection probability of birds with haemosporidian parasites differed among parasite genera: *Leucocytozoon* (13.2%, CI: 12.8 – 13.7%, n = 26,635 screened birds, intercept-only model), *Plasmodium* (12.8%, CI: 12.5 – 13.1%, n = 53,669), *Parahaemoproteus* (13.8%, CI: 13.5 – 14.1%, n = 53,669), and *Haemoproteus* (0.7%, CI: 0.6 – 0.8%, n = 53,669). Whereas the low overall infection probability for *Haemoproteus* can be explained by this genus being mostly restricted to Columbidae (doves and pigeons) and Fregatidae (frigatebirds), the similar infection probabilities for the other three haemosporidian

461 genera may reflect their ability to infect a broad spectrum of avian clades **(Supporting**
462 **Information Figure S3)**. Among the 141 avian host families surveyed, those with the highest
463 average infection probabilities were all songbirds (Passeriformes): Paridae, Corvidae, and
464 Oriolidae for *Leucocytozoon*; Zosteropidae and Melanocharitidae for *Parahaemoproteus*; and
465 Parulidae, Turdidae, and Conopophagidae for *Plasmodium*, according to the lower CI estimates
466 of phylogenetic effects (**Supporting Information Figure S3**).

467 Infection probabilities differed considerably among zoogeographical realms (**Figure 1,**
468 **Supporting Information Table S2)**. For the three most common haemosporidian genera
469 (*Leucocytozoon*, *Parahaemoproteus*, and *Plasmodium*) infection probabilities were highest in the
470 Saharo-Arabian realm, with lower CI estimates ≥ 24%. *Leucocytozoon* infection probabilities
471 were lowest in the Neotropical, Oceanian, and Panamanian realms. *Parahaemoproteus* infection
472 was lowest in the Australian, Neotropical, and Sino-Japanese realms. *Plasmodium* infection was
473 lowest in the Australian, Oceanian, Oriental, and Sino-Japanese realms (all respective upper CIs
474 < 10% from GLMMs with region as random effects, **Figure 1**). Given its restriction to doves and
475 frigatebirds, the prevalence of *Haemoproteus* was < 5% (respective upper CIs) in all realms
476 except for Oceanian and estimated to be highest in the Palearctic and Oceanian realms (both
477 lower CIs ≥ 2.3%).

478 We found considerable spatial variation in average infection probabilities across locations
479 within regions (GLMM with locations as random effects), although estimates with acceptable
480 uncertainty (credible intervals ≤ 10%) occurred in only 45 – 104 of the 1,630 sampling locations
481 (**Figure 2**). Using these location-based estimates, four currently recognisable local hotspots of
482 *Haemoproteus* infection were identified in the Neotropical realm, with infection rates exceeding
483 2% (respective lower CIs ≥ 2%). Hotspots (locations with highest lower CIs) for *Leucocytozoon*

484 and *Parahaemoproteus* were dispersed across different zoogeographical realms:
485 *Parahaemoproteus* in the Palearctic and Australian realms with lower CIs ≥ 25% and
486 *Leucocytozoon* in Afrotropical, Nearctic, and Palearctic with lower CIs ≥ 13%). Hotspots of
487 *Plasmodium* occurred in the Nearctic realm (three locations with lower CIs ≥ 21%).
488
489 ***Drivers of global infection probability***
490 Models that included phylogenetic and spatial effects and accounted for varying fixed-
491 effect coefficients (spatio-phyl-varcoef-GLMM, equation 5) provided the best fit to the observed
492 data and strongest predictive power according to both the DIC and CPO criteria (**Supporting**
493 **Information Table S3**). We therefore report results from this model unless stated otherwise. We
494 note however, that phylogenetic effects were burdened by high uncertainties, indicating the
495 challenges of disentangling phylogenetic effects from spatial and climatic covariates
496 (**Supporting Information Figure S3**).
497 Infection probabilities exhibited idiosyncratic associations with host traits, landscape
498 variables, and climate conditions at the global scale. Among the 14 covariates used in the
499 analyses, 11 exhibited 'global average' coefficient estimates for which CIs did not overlap with
500 zero (**Figure 3, Supporting Information Table S4**). As overall *Haemoproteus* prevalence was
501 extremely low (370 infections out 53,669 screened birds) and constrained to two host families
502 (Columbidae and Fregatidae), this parasite genus was not considered in the following analysis.
503 Local bird species richness showed a positive effect on infection probability for
504 *Leucocytozoon* (odds ratio, OR 1.83, CI 1.26 - 2.56) and *Parahaemoproteus* (OR 1.32, CI 1.09 -
505 1.59). Infection probability increased with increasing host body mass for *Leucocytozoon* (OR
506 1.25, CI 1.11 - 1.41), *Parahaemoproteus* (OR 1.62, CI 1.47 - 1.79), and *Plasmodium* (OR 1.36,

CI 1.24 - 1.48). Infection probability increased among bird species spending more time foraging in the canopy for *Leucocytozoon* (OR 1.13, CI 1.05 - 1.22) and *Parahaemoproteus* (OR 1.26, CI 1.18 - 1.35), but decreased for *Plasmodium* (OR 0.88, CI 0.81 - 0.95). *Leucocytozoon* infection probability increased with host migration distance (OR 1.19, CI 1.07 - 1.32). Higher proportions of wetland cover at different sites increased infection probability for *Plasmodium* (OR 1.35, CI 1.03 - 1.79), but decreased infection probability for *Parahaemoproteus* (OR 0.53, CI 0.37 - 0.78) and *Leucocytozoon* (OR 0.52, CI 0.29 - 0.95). Elevation increased infection probability for *Leucocytozoon* (OR 1.47, CI 1.14 - 1.9), but decreased infection probability for *Plasmodium* (OR 0.65, CI 0.53 - 0.80). Infection probability for *Leucocytozoon* (OR 0.33, CI 0.20 - 0.53) was considerably lower at sites with higher rainfall during the driest month and decreased with increasing rainfall seasonality (OR 0.59, CI 0.43 - 0.80). At locations with higher annual rainfall, infection probability increased for *Leucocytozoon* (OR 1.83, CI 1.15 - 2.91), but decreased for *Plasmodium* (OR 0.75, CI 0.58 - 0.97). Sites with higher proportions of forest cover and vegetation density exhibited increased probability of infection by *Parahaemoproteus* (OR 1.31, CI 1.02 - 1.70) and *Plasmodium* (OR 1.44, CI 1.05 - 1.97), respectively. Annual mean temperature, annual fluctuation in vegetation density, and distance to equator showed no evident covariation with infection probability (i.e., CIs overlapped with zero) for any of the three parasite genera (**Figure 3**).

Varying coefficient estimates revealed that several covariate effects, notably mostly host ecological traits rather than environmental predictors, differed across zoogeographical realms (see **Supporting Information Table S5** for variance estimates in coefficients). Two host traits and one environmental driver exhibited opposing effects on the probability of parasite infection across zoogeographical realms: local bird species richness had a positive effect on infection

probability for *Parahaemoproteus* in the Afrotropical, Palearctic, and Sino-Japanese realms and a negative effect in the Saharo-Arabian realm (**Figure 4**). Migration distance was associated with increased *Parahaemoproteus* infection probability in the Neotropical, Saharo-Arabian, and Sino-Japanese realms, but with decreased infection probability in the Nearctic and Oriental realms (**Figure 4**). Likewise, migration distance was associated with increased *Plasmodium* infection in the Neotropical, Oceanian, and Oriental realms, but with decreased infection probability in the Nearctic realm (**Figure 4**). Annual fluctuation in vegetation density was associated with increased infection with *Leucocytozoon* in the Nearctic realm but with decreased infection in the Palearctic realm (**Figure 4**). In addition, host body mass (infection with *Leucocytozoon* and *Parahaemoproteus*), canopy foraging frequency (infection with *Parahaemoproteus* and *Plasmodium*), and proportion of wetland cover (infection with *Leucocytozoon*), all varied across realms according to variance in coefficient estimates (**Figure 4, Supporting Information Table S5)**.

Discussion

Understanding large-scale variation in parasite prevalence and spread is of increasing importance in a changing world, where counteracting disease emergence and outbreaks pose a global challenge. Using a global database of infections by four genera of a cosmopolitan group of vector-transmitted blood parasites of birds, we show that infection probabilities for each parasite genus vary considerably across zoogeographic realms and avian host families. Our hierarchical global analysis identified key drivers of infection probability that differed in their magnitudes and directions among parasite genera. In particular, we found that bird richness and host attributes may have rather different impacts on infection risk in different zoogeographical

553 realms, whereas climate and habitat conditions are more likely to influence infection risk
554 consistently across zoogeographical realms. Multiple global hotspots of avian haemosporidian
555 infection emerge from our results with strong variation in infection probabilities within realms,
556 indicating that prevalence in avian hosts responds to regional factors as well as broad-scale
557 global drivers such as latitudinal ecological/climatic gradients. Accounting for environmental
558 context in synergy with biotic drivers, such as species ecological traits and host species assembly
559 patterns, is critical for understanding variation in infection probability and conditions that enable
560 parasites to spread.
561
562 ***Hotspots of haemosporidian infection probability***
563 Disease hotspots are not necessarily stable over time and may result from high frequency
564 of local spillover event from alternative hosts species. A key challenge in disease ecology is to
565 identify traits of alternative host species (phylogenetically related or not) that might make them
566 competent reservoirs of pathogens and increase local prevalence (Jones et al., 2008). Here we
567 identified locations with the greatest infection risk of a vector-transmitted parasite and host traits
568 that potentially increase local prevalence. Notably, our macroecological analyses of infection
569 probability identified hotspots for haemosporidian parasites dispersed across different
570 zoogeographical regions, some well outside the known biodiversity hotspots for most free-living
571 organisms in the tropics. Unlike the pantropical distribution of human malaria hotspots, our map
572 on global infection risk depicts hotspots for avian malaria in the Nearctic region and for
573 *Parahaemoproteus*, a related avian malaria parasite, in the Palearctic region.
574 The longstanding and much-debated hypothesis that infection risk increases toward the
575 equator (Jones et al., 2008; Stephens et al., 2016, Allen et al., 2017) was not supported in our

synthesis for vector-transmitted parasites. Tropical regions support higher bird diversity in comparison to temperate regions (Duchêne & Cardillo, 2015), and thus haemosporidian parasites from tropical regions may have a higher diversity of available "niches" to exploit. Furthermore, the greater diversity of both avian and vector host species in the tropics could lead to increased diversity within individual hosts through lineage sharing and host shifting (Ricklefs et al., 2014). While surprising, the observed absence of a latitudinal gradient in infection probability for the three most prevalent haemosporidian parasites matches what was found for lineage diversity at a global scale (Clark, 2018). Clark (2018) demonstrated that more diverse communities of haemosporidian parasites do not necessarily occur in tropical regions and suggested that macroevolutionary factors, such as propensity of parasites to shift hosts locally, or timing of diversification, are more important drivers of local parasite diversity. Whether haemosporidian prevalence is correlated with lineage diversity and the propensity of these parasites to shift among hosts at different rates across latitude has yet to be investigated.

Our findings suggests that haemosporidian infection probabilities emerge not only from general global drivers such as climate, avian host richness, and, possibly, migratory flyways that determine macroecological patterns of community assembly, but also from region-scale habitat and climate variation.

Spatial distribution of avian hosts overshadows phylogenetic signal in infection probability

Host phylogenetic position has been associated with variation in haemosporidian prevalence in avian communities and host clades (Barrow et al., 2019; Clark et al., 2020). Our study confirms these previous findings in terms of a strong phylogenetic signal in bird infection patterns with haemosporidian parasites. However, after accounting for both phylogeny and the

location of the collected samples, we found considerable uncertainty in the phylogenetic signal at a global scale, indicating that strong phylogenetic signal inferred from a pooled sample (i.e., without taking spatial context/covariance into account) can be misleading. This uncertainty in phylogenetic signal can be especially pronounced at a large scale, in which distinct local host assemblages and samples are likely to include closely related individuals/species, which in turn may generate phylogenetic 'pseudoreplicates' at the same locations.

Recognizing that avian haemosporidian prevalence is highly variable within and among host clades, and that it is spatially clustered, as we have shown here, provides a new framework for outlining region-specific predictions of infection risk by multi-host vector-transmitted parasites. This is particularly true for areas undergoing rapid climate change, anthropogenic landscape transformation, and shifting host species assemblages. We believe that these patterns point to strong synergistic effects of host traits, landscape features, and climatic filters driving infection patterns.

Idiosyncratic drivers influence differences in global infection risk among haemosporidian genera

A central finding of our analysis was not only the identification of host traits driving infection probability for the three most prevalent haemosporidian genera, but also how their effects vary across zoogeographic realms. We showed that bird species which migrate longer distances are more likely to be infected by *Leucocytozoon* worldwide. As most long-distance migrants spend part of their annual cycle breeding in temperate regions, where black fly vectors are more diverse and abundant (Currie & Adler, 2008), there would be much higher potential for *Leucocytozoon* transmission in long-distance migrants than in resident tropical species.

Migration distance influenced infection probability in opposing directions across zoogeographical realms for the genera *Plasmodium* and *Parahaemoproteus* (see results and Figure 4). These inverse trends in infection risk for vector transmitted parasites in response to migration patterns warrant future research into underlying mechanisms. Perhaps one of the interesting aspects to consider (if relevant data become available) could be the spatial context of parasites transmission, given the possibility that transmission in migratory birds may take either place in the wintering or breeding area but not necessarily in both. This is especially relevant given the multifaceted environmental changes, which are likely to amplify the anticipated changes in bird migration and community assembly (Visser et al., 2009; Howard et al., 2020) and hence the future infection risk with haemosporidian parasites.

Avian hosts inhabiting sites with a higher proportion of wetland cover and denser vegetation are at greater risk of *Plasmodium* infection. The probability of a bird being infected with *Parahaemoproteus* consistently increased with proportion of forest cover, while it decreased in sites with higher proportions of wetland cover. When anthropogenic landscape changes create structures capable of collecting rainwater (e.g., artificial lakes, mining pits, rice fields) or change the course or flooding regime of rivers (e.g., dams, irrigation systems), such changes in water availability may increase infection of birds with avian. Conversely, reduction in forest cover may diminish the local transmission of *Plasmodium* and *Parahaemoproteus* among avian hosts, but whether tree cover removal has a direct effect on vector capacity or parasite capacity to shift between hosts at large spatial scales has yet to be investigated.

We found that higher annual rainfall is associated with decreased prevalence of *Plasmodium* but increased prevalence of *Leucocytozoon.* Furthermore, *Leucocytozoon* infection risk decreases at sites with substantial rainfall during the driest months and sites with pronounced

variation in rainfall throughout the year. The relationship between rainfall and prevalence suggests that the expected disruption of precipitation patterns due to anthropogenic impacts on global climate (Wehner, 2020) may affect prevalence of avian haemosporidian genera differentially in the future. The magnitude of this impact may vary by region owing to biogeographic structure in realized host specialization of haemosporidian lineages (Fecchio et al., 2019).

Elevation emerged as a predictor of *Plasmodium* and *Leucocytozoon* infection probability at a global scale, although with an opposite effect for each parasite genus. Our global dataset allowed us to determine the probability of a bird being infected across an elevation gradient ranging from sea level to ~ 4,700 meters elevation across 10 zoogeographic realms, while simultaneously controlling for other climatic characteristics known to constrain vector development, activity, and abundance (e.g., temperature and moisture level), as well as parasite reproduction (temperature). This approach consistently demonstrated that the probability of an individual bird being infected with *Plasmodium* decreases with elevation across the globe, presumably because of constraints in parasite development and transmission by mosquito vectors at higher elevation sites (Atkinson et al., 2014). Although we showed that *Leucocytozoon* infection probability increased with elevation, presumably owing to the affinity of black fly vectors for colder sites at high elevations, hotspots of *Leucocytozoon* prevalence were also scattered across lowland bird assemblages.

Generally, with the currently available empirical evidence being mostly constraint to vertebrate host infections, correlative approaches as employed in this study allow limited insights into which species and interactions in the vertebrate-host-pathogen transmission cycle are most sensitive to environmental change, warranting future research into specific host-vector

associations and host preferences. This is especially relevant for ectothermic arthropod vectors, for which host preferences and biting rates are sensitive to climate and land use changes (Rose et al., 2020).

Conclusions

Our spatio-phylogenetic analysis revealed that infection probability of haemosporidian parasites varies across zoogeographical realms and avian host clades owing to broad-scale and possibly also regional-scale variation in environmental conditions and host assemblages. A novel aspect of our study was to determine the drivers and hotspots of infection probability for each haemosporidian genus on a global scale rather than at population or community levels. Importantly, we found that infections in some low-prevalence realms were disproportionately concentrated in local hotspots, suggesting that regional-scale modifications in habitat and microclimate (and perhaps also the way host species assemble in response to strong habitat modification) may increase transmission at a regional scale. However, the synergistic effect of environmental drivers, such as precipitation, vegetation density, and proportion of forest and wetland cover, along with host community and assembly attributes on prevalence of multi-host pathogens across realms, underscores the importance of considering biogeographic patterns in host-parasite systems. At the same time, we suggest that the scattered distribution of local infection hotspots demonstrates that local processes, such as strong habitat modification and the resulting shifts in host species assemblages, can produce unexpected increases in parasite prevalence, emphasising that disease outbreak may be difficult to predict from generalizable large-scale patterns such as climate alone.

691 **Literature cited**

692 Allen, T., Murray, K. A., Zambrana-Torrelio, C., Morse, S. S., Rondinini, C., Di Marco, M., ...
693 Daszak, P. (2017). Global hotspots and correlates of emerging zoonotic diseases. Nature
694 Communications, (8), 1124. https://doi.org/10.1038/s41467-017-00923-8

695 Altizer, S., Ostfeld, R. S., Johnson, P. T., Kutz, S., & Harvell, C. (2013). Climate change and
696 infectious diseases: from evidence to a predictive framework. Science, 341(6145), 514-519.
697 doi: 10.1126/science.1239401

698 Atkinson, C. T., Utzurrum, R. B., Lapointe, D. A., Camp, R. J., Crampton, L. H., Foster, J. T., &
699 Giambelluca, T. W. (2014). Changing climate and the altitudinal range of avian malaria in
700 the Hawaiian Islands - an ongoing conservation crisis on the island of Kaua'i. Global
701 Change Biology, 20(8), 2426-2436. doi: 10.1111/gcb.12535

702 Bakka, H., Rue, H., Fuglstad, G.-A., Riebler, A., Bolin, D., Illian, J., … Lindgren, F. (2018).
703 Spatial modeling with R-INLA: A review. WIREs Computational Statistics, 10(6), e1443.
704 https://doi.org/10.1002/wics.1443

705 Barrow, L. N., McNew, S. M., Mitchell, N., Galen, S. C., Lutz, H. L., Skeen, H., … Witt, C. C.
706 (2019). Deeply conserved susceptibility in a multi-host, multi-parasite system. Ecology
707 Letters, 22(6), 987-998. doi:10.1111/ele.13263

708 Benning, T. L., LaPointe, D., Atkinson, C. T., & Vitousek, P. M. (2002). Interactions of climate
709 change with biological invasions and land use in the Hawaiian Islands: Modeling the fate of
710 endemic birds using a geographic information system. Proceedings of the National Academy
711 of Sciences of the United States of America, 99 (22), 14246-14249. doi
712 10.1073/pnas.16237239

713 Bensch, S., Hellgren, O., & Pérez-Tris, J. (2009). MalAvi: a public database of malaria parasites
714 and related haemosporidians in avian hosts based on mitochondrial cytochrome b lineages.
715 Molecular Ecology Resources, 9(5), 1353-1358. doi: 10.1111/j.1755-0998.2009.02692.x
716 Cable, J., Barber, I., Boag, B., Ellison, A. R., Morgan, E. R., Murray, K., … Booth, M. (2017).
717 Global change, parasite transmission and disease control: lessons from ecology.
718 Philosophical Transactions of the Royal Society of London. Series B, Biological sciences,
719 372(1719), 20160088. https://doi.org/10.1098/rstb.2016.0088
720 Canard, E. F., Mouquet, N., Mouillot, D., Stanko, M., Miklisova, D., & Gravel, D. (2014).
721 Empirical evaluation of neutral interactions in host-parasite networks. American Naturalist,
722 183(4), 468-479. doi: 10.1086/675363
723 Christensen, J. H., Hewitson, B., Busuioc, A., Chen, A., Gao, X., Held, I., … Whetton, P. (2007).
724 Regional Climate Projections. In: Solomon, S., Qin, D., Manning, M., Chen, Z., Marquis, M.,
725 Averyt, K. B… Miller, H. L. (Eds.), *Climate Change 2007: The Physical Science Basis.*
726 *Contribution of Working Group I to the Fourth Assessment Report of the Intergovernmental*
727 *Panel on Climate Change* (Vol. 1, pp. 847-940). New York, NY: Cambridge University
728 Press.
729 Clark, N. J. (2018). Phylogenetic uniqueness, not latitude, explains the diversity of avian blood
730 parasite communities worldwide. Global Ecology and Biogeography, 27(6), 744-755.
731 https://doi.org/10.1111/geb.12741
732 Clark, N. J., Drovetski, S. V., & Voelker, G. (2020). Robust geographical determinants of
733 infection prevalence and a contrasting latitudinal diversity gradient for haemosporidian
734 parasites in Western Palearctic birds. Molecular Ecology, 29(16), 3131-3143.
735 https://doi.org/10.1111/mec.15545

736 Currie, D. C., & Adler, P. H. (2008). Global diversity of black flies (Diptera: Simuliidae) in
737 freshwater. Hydrobiologia, 595, 469-475. doi: 10.1007/s10750-007-9114-1
738 de Angeli Dutra, D., Fecchio, A., Braga, É. M., & Poulin, R. (2021). Migratory birds have higher
739 prevalence and richness of avian haemosporidian parasites than residents. International
740 Journal for Parasitology. https://doi.org/10.1016/j.ijpara.2021.03.001
741 Duchêne, D. A., & Cardillo, M. (2015). Phylogenetic patterns in the geographic distributions of
742 birds support the tropical conservatism hypothesis. Global Ecology and Biogeography,
743 24(11), 1261-1268. https://doi.org/10.1111/geb.12370
744 Dufour, P., Descamps, S., Chantepie, S., Renaud, J., Guéguen, M., Schiffers, K., Thuiller, W., &
745 Lavergne, S. (2020). Reconstructing the geographic and climatic origins of long-distance bird
746 migrations. Journal of Biogeography, 47(1), 155-166. https://doi.org/10.1111/jbi.13700
747 Ellis, V. A., Fecchio, A., & Ricklefs, R. E. (2020). Haemosporidian parasites of Neotropical
748 birds: Causes and consequences of infection. The Auk, 137(4), ukaa055.
749 https://doi.org/10.1093/auk/ukaa055
750 Fecchio, A., Bell, J. A., Bosholn, M., Vaughan, J. A., Tkach, V. V.., Lutz, H. L., … Clark, N. J.
751 (2020). An inverse latitudinal gradient in infection probability and phylogenetic diversity for
752 *Leucocytozoon* blood parasites in New World birds. Journal of Animal Ecology, 89(2), 423-
753 435. https://doi.org/10.1111/1365-2656.13117
754 Fecchio, A., Wells, K., Bell, J. A., Tkach, V. V., Lutz, H. L., Weckstein, J. D., … Clark, N. J.
755 (2019). Climate variation influences host specificity in avian malaria parasites. Ecology
756 Letters, 22(3), 547–557. doi: 10.1111/ele.13215
757 Ferraguti, M., Hernández-Lara, C., Sehgal, R. N. M., & Santiago-Alarcon, D. (2020).
758 Anthropogenic effects on avian haemosporidians and their vectors. In D. Santiago-Alarcon &

759 A. Marzal (Eds.), *Avian malaria and related parasites in the tropics – ecology, evolution and*
760 *systematics* (pp. 451-485). Cham, Switzerland: Springer.
761 Fick, S. E., & Hijmans, R. J. (2017). WorldClim 2: new 1-km spatial resolution climate surfaces
762 for global land areas. International Journal of Climatology, 37(12), 4302-4315.
763 doi:10.1002/joc.5086
764 Filion, A., Eriksson, A., Jorge, F., Niebuhr, C. N., & Poulin, R. (2020). Large-scale disease
765 patterns explained by climatic seasonality and host traits. Oecologia, 194(4), 723–733.
766 https://doi.org/10.1007/s00442-020-04782-x
767 Fischer, E. M., Lawrence, D. M., & Sanderson, B. M. (2011). Quantifying uncertainties in
768 projections of extremes - a perturbed land surface parameter experiment. Climate Dynamics,
769 37, 1381–1398. https://doi.org/10.1007/s00382-010-0915-y
770 Galen, S. C., Borner, J., Martinsen, E. S., Schaer, J., Austin, C. C., West, C. J., & Perkins, S. L.
771 (2018). The polyphyly of *Plasmodium*: comprehensive phylogenetic analyses of the malaria
772 parasites (order Haemosporida) reveal widespread taxonomic conflict. Royal Society Open
773 Science, 5, 171780. http://dx.doi.org/10.1098/rsos.171780
774 Garvin, M. C., & Greiner, E. C. (2003). Ecology of *Culicoides* (Diptera: Ceratopogonidae) in
775 southcentral Florida and experimental *Culicoides* vectors of the avian hematozoan
776 *Haemoproteus danilewskyi* Kruse. Journal of Wildlife Diseases, 39, 170–178. doi:
777 10.7589/0090-3558-39.1.170
778 Gupta, P., Vishnudas, C. K., Robin, V. V., & Dharmarajan, G. (2020). Host phylogeny matters:
779 Examining sources of variation in infection risk by blood parasites across a tropical montane
780 bird community in India. Parasites and Vectors, 13, 536. https://doi.org/10.1186/s13071-020-
781 04404-8

Howard, C., Stephens, P. A., Pearce-Higgins, J. W., Gregory, R. D., Butchart, S. H. M., & Willis, S. G. (2020). Disentangling the relative roles of climate and land cover change in driving the long-term population trends of European migratory birds. Diversity and Distributions, 26(11), 1442-1455. https://doi.org/10.1111/ddi.13144

Harvey, J. A., & Voelker, G. (2019). Host associations and climate influence avian haemosporidian distributions in Benin. International Journal for Parasitology, 49(1), 27-36. https://doi.org/10.1016/j.ijpara.2018.07.004

Holt, B. G., Lessard, J-P., Borregaard, M. K., Fritz, S. A., Araújo, M. B., Dimitrov, D., … Rahbek, C. (2013). An update of Wallace's zoogeographic regions of the World. Science, 339(6115), 74-78. doi: 10.1126/science.1228282

Ishtiaq, F., Bowden, C. G. R., & Jhala, Y. V. (2017). Seasonal dynamics in mosquito abundance and temperature do not influence avian malaria prevalence in the Himalayan foothills. Ecology and Evolution, 7(19), 8040-8057. https://doi.org/10.1002/ece3.3319

Jetz, W., Thomas, G. H., Joy, J. B., Hartmann, K., & Mooers, A. O. (2012). The global diversity of birds in space and time. Nature, 491, 444-448. https://doi.org/10.1038/nature11631

Jones, K. E., Patel, N. G., Levy, M. A., Storeygard, A., Balk, D., Gittleman, J. L., & Daszak P. (2008). Global trends in emerging infectious diseases. Nature, 451(7181), 990-993. https://doi.org/10.1038/nature06536

Lafferty, K. D. (2009). The ecology of climate change and infectious diseases. Ecology, 90(4), 888–900. https://doi.org/10.1890/08-0079.1

Lindgren, F., Rue, H., & Lindstrøm, J. (2011). An explicit link between Gaussian fields and Gaussian Markov random fields: the stochastic partial differential equation approach. Journal

804 of the Royal Statistical Society: Series B (Statistical Methodology), 73(4), 423-498.
805 doi:10.1111/j.1467-9868.2011.00777.x
806 Loiseau, C., Harrigan, R. J., Bichet, C., Julliard, R., Garnier, S., Lendvai, A. Z., Chastel, O., &
807 Sorci, G. (2013). Predictions of avian *Plasmodium* expansion under climate change.
808 Scientific Reports, 3, 1126. doi: 10.1038/srep01126
809 Loiseau, C., Harrigan, R. J., Cornel, A. J., Guers, S. L., Dodge, M., Marzec, T., … Sehgal, R. N.
810 M. (2012). First evidence and predictions of *Plasmodium* transmission in Alaskan bird
811 populations. PLoS ONE, 7(9), e44729. https://doi.org/10.1371/journal.pone.0044729
812 Lutz, H. L., Hochachka, W. M., Engel, J. I., Bell, J. A., Tkach, V. V., Bates, J. M., … Weckstein,
813 J. D. (2015). Parasite prevalence corresponds to host life history in a diverse assemblage of
814 Afrotropical birds and haemosporidian parasites. PLoS ONE, 10(4), e0121254.
815 https://doi.org/10.1371/journal.pone.0121254
816 Minias, P. (2019). Evolution of heterophil/lymphocyte ratios in response to ecological and life-
817 history traits: A comparative analysis across the avian tree of life. Journal of Animal
818 Ecology, 88(4), 554-565. https://doi.org/10.1111/1365-2656.12941
819 Mordecai, E. A., Paaijmans, K. P., Johnson, L. R., Balzer, C., Ben-Horin, T., de Moor, E., …
820 Lafferty, K. D. (2013). Optimal temperature for malaria transmission is dramatically lower
821 than previously predicted. Ecology Letters, 16(1), 22-30. doi:10.1111/ele.12015
822 Mordecai, E. A., Ryan, S. J., Caldwell, J. M., Shah, M. M., & LaBeaud, A. D. (2020). Climate
823 change could shift disease burden from malaria to arboviruses in Africa. The Lancet
824 Planetary Health, 4(9), e416-e423. https://doi.org/10.1016/S2542-5196(20)30178-9
825 Paradis, E., Claude, J., & Strimmer, K. (2004). APE: Analyses of phylogenetics and evolution in
826 R language. Bioinformatics, 20(2), 289–290. https://doi.org/10.1093/bioinformatics/btg412

827 Pérez-Rodríguez, A., de la Hera, I., Fernández-González, S., & Pérez-Tris, J. (2014). Global
828 warming will reshuffle the areas of high prevalence and richness of three genera of avian
829 blood parasites. Global Change Biology, 20(8), 2406-2416.
830 https://doi.org/10.1111/gcb.12542
831 Ricklefs, R. E., Outlaw, D. C., Svensson-Coelho, M., Medeiros, M. C. I., Ellis, V. A., & Latta, S.
832 (2014). Species formation in avian malaria parasites. Proceedings of the National Academy
833 of Sciences of the United States of America, 111(41), 14816-14821.
834 https://doi.org/10.1073/pnas.1416356111
835 Rose, N. H., Sylla, M., Badolo, A., Lutomiah, J., Ayala, D., Aribodor, O. B., … McBride, C. S.
836 (2020). Climate and urbanization drive mosquito preference for humans. Current Biology,
837 30(18), 3570-3579. https://doi.org/10.1016/j.cub.2020.06.092
838 Rue, H., Martino, S., & Chopin, N. (2009). Approximate Bayesian inference for latent Gaussian
839 models by using integrated nested Laplace approximations. Journal of the Royal Statistical
840 Society: Series B (Statistical Methodology), 71(2), 319-392. https://doi.org/10.1111/j.1467-
841 9868.2008.00700.x
842 Ruhs, E. C., Martin, L. B., & Downs, C. J. (2020). The impacts of body mass on immune cell
843 concentrations in birds. Proceedings of the Royal Society B: Biological Sciences, 287,
844 20200655. http://dx.doi.org/10.1098/rspb.2020.0655
845 Ryan, S. J., Carlson, C. J., Mordecai, E. A., & Johnson, L. R. (2019). Global expansion and
846 redistribution of *Aedes*-borne virus transmission risk with climate change. PLoS Neglected
847 Tropical Diseases, 13(3), e0007213. https://doi.org/10.1371/journal.pntd.0007213
848 Santiago-Alarcon, D., MacGregor-Fors, I., Falfán, I., Lüdtke, B., Segelbacher, G., Schaefer, H.
849 M., & Renner, S. (2019). Parasites in space and time: a case study of haemosporidian

spatiotemporal prevalence in urban birds. International Journal for Parasitology, 49(3-4), 235-246. doi: 10.1016/j.ijpara.2018.08.009.

Santiago-Alarcon, D., Palinauskas, V., & Schaefer, H. M. (2012). Diptera vectors of avian haemosporidian parasites: untangling parasite life cycles and their taxonomy. Biological Reviews, 87(4), 928-964. doi: 10.1111/j.1469-185X.2012.00234.x

Simpson, D., Rue, H., Riebler, A., Martins, T.G., & Sørbye, S. H. (2017). Penalising model component complexity: a principled, practical approach to constructing priors. Statistical Science, 32(1), 1-28. doi:10.1214/16-STS576

Spiegelhalter, D. J., Best, N. G., Carlin, B. P., & van der Linde, A. (2002). Bayesian measures of model complexity and fit. Journal of the Royal Statistical Society: Series B (Statistical Methodology), 64(4), 583-639. https://doi.org/10.1111/1467-9868.00353

Stephens, P. R., Altizer, S., Smith, K. F., Alonso Aguirre, A., Brown, J. H., Budischak, S. A., … Poulin, R. (2016). The macroecology of infectious diseases: a new perspective on global-scale drivers of pathogen distributions and impacts. Ecology Letters, 19(9), 1159-1171. doi: 10.1111/ele.12644

Valkiūnas, G. (2005). *Avian malaria parasites and other haemosporidia* (2nd ed.). Boca Raton, FL: CRC Press.

Visser, M. E., Perdeck, A.C., van Balen, J. H., & Both, C. (2009). Climate change leads to decreasing bird migration distances. Global Change Biology, 15(8), 1859-1865. https://doi.org/10.1111/j.1365-2486.2009.01865.x

Wehner, M. F. (2020). Characterization of long period return values of extreme daily temperature and precipitation in the CMIP6 models: Part 2, projections of future change. Weather and Climate Extremes, 30, 100284. https://doi.org/10.1016/j.wace.2020.100284

873 Weiss, D. J., Lucas, T. C. D., Nguyen, M., Nandi, A. K., Bisanzio, D., Battle, K. E., … Gething,
874 P. W. (2019). Mapping the global prevalence, incidence, and mortality of *Plasmodium*
875 *falciparum*, 2000-17: a spatial and temporal modelling study. Lancet, 394(10195), 322-331.
876 doi: 10.1016/S0140-6736(19)31097-9
877 Wells, K., & Clark, N. J. (2019). Host specificity in variable environments. Trends in
878 Parasitology, 35(6), 452-465. https://doi.org/10.1016/j.pt.2019.04.001
879 Williams, B. A., Venter, O., Allan, J. R., Atkinson, S. C., Rehbein, J. A., Michelle Ward, M., …
880 Watson, J. E. M. (2020). Change in terrestrial human footprint drives continued loss of intact
881 ecosystems. One Health, 3, 371–382. https://doi.org/10.1016/j.oneear.2020.08.009
882 Wilman, H., Belmaker, J., Simpson, J., de la Rosa, C., Rivadeneira, M. M., & Jetz, W. (2014).
883 EltonTraits 1.0: Species-level foraging attributes of the world's birds and mammals. Ecology,
884 95(7), 2027-2027. doi: 10.1890/13-1917.1
885

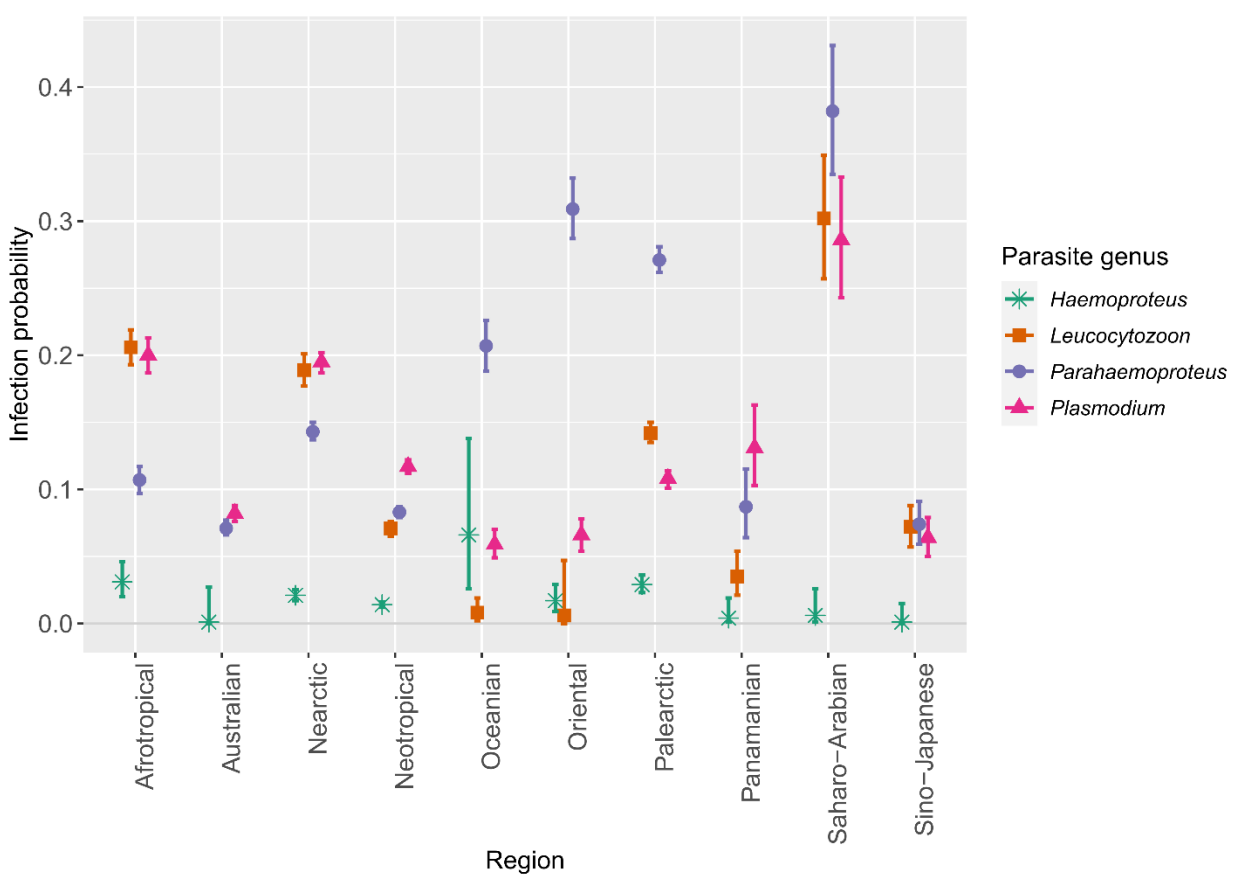

886

887 **Figure 1.** Region-specific estimates of average infection probabilities of birds for four

888 haemosporidian genera, based on 53,669 sampled bird individuals (estimates from GLMM with

889 region as a random effect). Error bars depict 95% credible intervals, reflecting uncertainty

890 related to sample sizes in different regions.

891

892

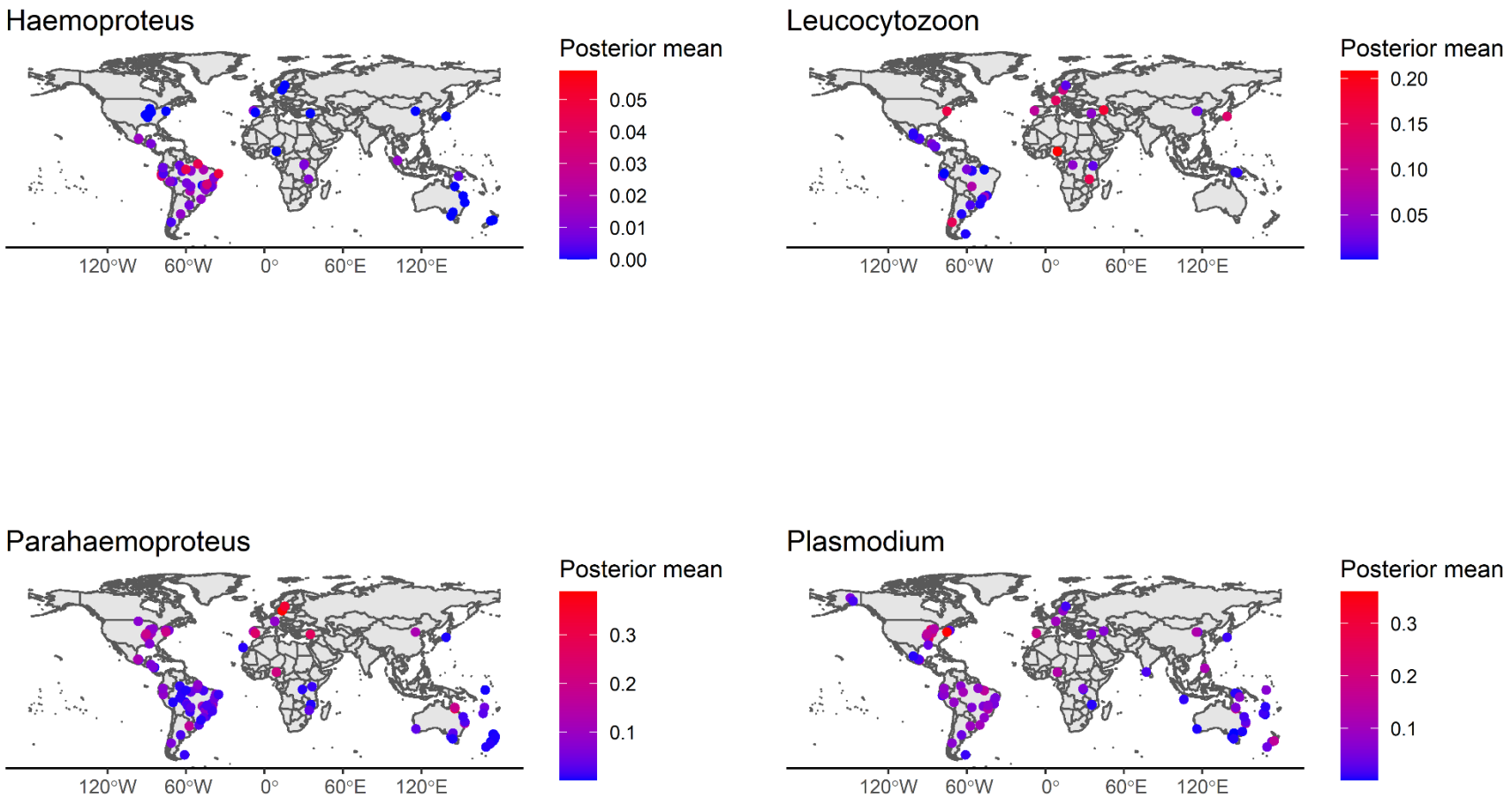

893

894 **Figure 2.** Estimated average parasite prevalence at different locations, shown only for locations with ≤ 10% uncertainty in estimates

895 according to the size of 95% credible intervals.

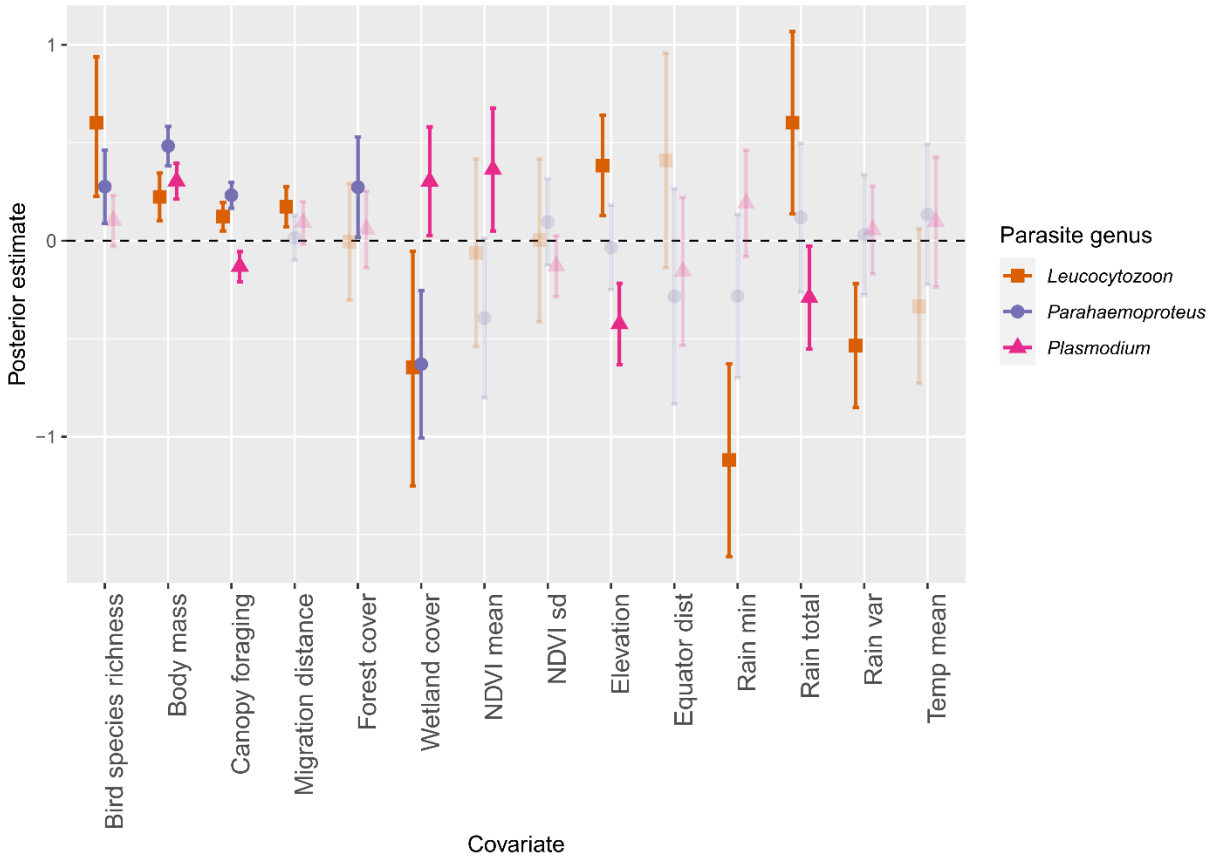

Figure 3. Estimates of the 'global average' effects of different drivers on variation in the infection probability of the three most common avian haemosporidian genera (based on scaled covariates). Points depict posterior means of the fixed effect estimates from a spatio-phylogenetic varying coefficient model, and vertical lines indicate 95% credible intervals. For each parasite genus, the covariates that overlap with zero are shown in light bars.

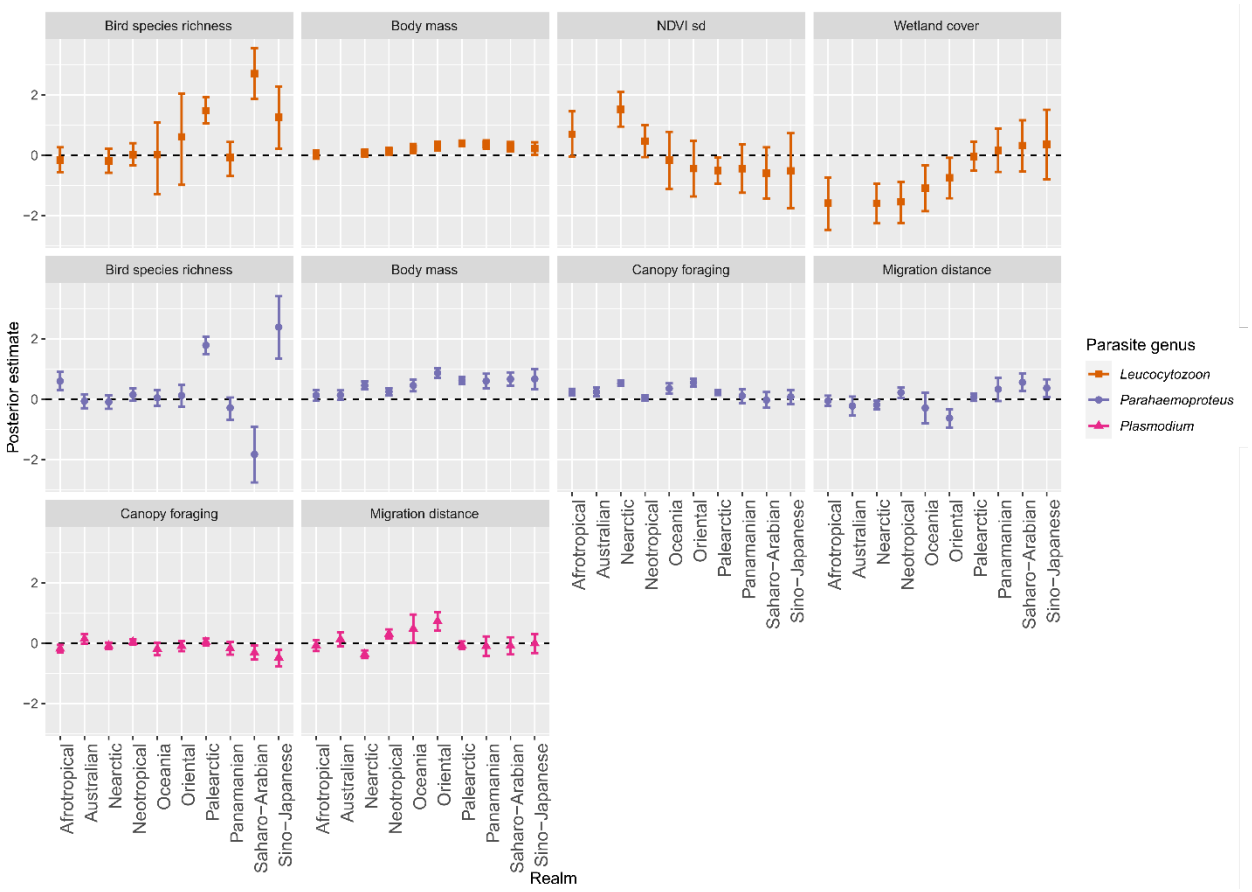

908

909 **Figure 4.** Varying coefficient estimates for variables with distinct effects across zoogeographical
910 realms. Points depict the posterior mean of the regional-level effect estimates from a spatio-
911 phylogenetic varying coefficient model, and vertical lines indicate 95% credible intervals.

912

913

914

915

916

917

918